Evidence of Relaxation and Spontaneous Transition to a High-Confinement State in High-β Steady-State Plasmas Sustained by Rotating Magnetic Fields

H. Y. Guo, A. L. Hoffman, L. C. Steinhauer, K. E. Miller, and R. D. Milroy

Redmond Plasma Physics Laboratory, University of Washington, Seattle, Washington 98195, USA

(Received 30 August 2006; published 6 December 2006)

Evidence of relaxation has appeared, for the first time, in the extremely high-β, steady-state field-reversed configuration plasma states driven by rotating magnetic fields (RMF) in the translation, confinement, and sustainment experiment. The plasma self-organizes into a near-force-free state in the vicinity of the magnetic axis, with significant improvement in confinement. Associated with this change in magnetic topology is the appearance of an axial RMF component; this would, in turn, generate a current drive in the poloidal direction, thus sustaining the magnetic helicity. A newly developed two-dimensional ''equilibrium-lite'' model is employed to analyze the magnetic properties of the final high-confinement state, and shows a large q and a significant magnetic shear in the core.

DOI: 10.1103/PhysRevLett.97.235002 PACS numbers: 52.55.Lf, 52.35.Py, 52.55.Dy, 52.55.Wq

Relaxation in low-β plasma states, such as solar and space plasmas, as well as laboratory plasmas including spheromaks and reversed field pinches, has long been recognized and is usually described in terms of the Taylor relaxation principle [1]. The Taylor theory predicts force-free plasma states with $\nabla \times \mathbf{B} = \lambda \mathbf{B}$, where λ is a global constant. However, these theoretical states have intrinsically $\beta = 0$. Recognizing that realistic plasmas have finite β, more general relaxation principles [2,3] have been advanced, but none of these has been verified by experiment. Recently, strong evidence for relaxation in an extremely high-β (over 85%) field-reversed configuration (FRC) plasma state has been obtained from the translation, confinement, and sustainment (TCS) experiment [4]. This high-β plasma state was produced by highly super-Alfvénic translation of a spheromaklike plasmoid produced by the conventional θ-pinch technology. The initial plasmoid in translation had little poloidal field, but strong, oppositely directed toroidal fields at its ends. After extremely violent reflections from the magnetic mirrors at the ends of the confinement chamber, the plasmoid quickly relaxes into a spherical-torus-like FRC state [5].

The θ-pinch formed or translated FRCs are, however, limited to relatively low magnetic flux and sub-ms lifetimes. TCS has recently demonstrated, for the first time, formation and steady-state sustainment of flux-confined, elongated FRCs for up to 100 resistive decay times, using rotating magnetic fields (RMF) [6]. New evidence of relaxation has appeared in this long pulse operation, as signified by the self-generation of a significant toroidal field, with spontaneous transition to a high-confinement state. Further investigation of high time and spatial resolution magnetic measurements reveals that the transition occurs at the onset of a *double* low-frequency drift (LFD) mode [7], arising from the bifurcation of electron drifts. The basic RMF structure changes dramatically during the transition; a new axial RMF $\tilde{b}_z$ field appears. This, along with the normal RMF $\tilde{b}_r$ and $\tilde{b}_\theta$, generates current drive in both toroidal and *poloidal* directions. The latter would serve to sustain the magnetic helicity. The final *relaxed* state exhibits the following key properties: (1) a near-force-free state in the core region, (2) a large $q \sim 1$ along with significant magnetic shear near the magnetic axis, and (3) significantly improved confinement. This Letter presents these results.

RMF has been investigated for many years as a current-drive technique [8,9] initially through a long series of rotamak experiments at Flinders University in Australia [10]. RMF was subsequently adopted as both a FRC formation and current sustainment technology in TCS [11]. In the basic RMF current-drive scheme for an elongated FRC, RMF imposes a time averaged Hall force $\langle \tilde{j}_z \tilde{b}_r \rangle$ on the electron fluid, driving a steady toroidal current and sustaining the configuration. RMF also produces a radial inward force $\langle \tilde{j}_z \tilde{b}_\theta \rangle$ due to the interaction of the electron oscillation with the azimuthal component of the RMF. This force not only contributes to the radial equilibrium, supplementing the magnetic pressure gradient $\nabla(B_z^2/2\mu_o)$, but can also provide stabilization against the potentially disruptive $n = 2$ rotating interchange mode [12].

Recently, a significant new phenomenon has appeared in TCS when the FRC sustainment time was extended to the full 10-ms pulse length of the RMF power supply (~ 100 resistive decay times), i.e., spontaneous transition to a high-confinement state marked by a sudden increase in the external poloidal field [6]. This event was accompanied by the self-generation of a small toroidal field. Following this intriguing discovery, we have further investigated the dynamics of the transition and detailed mode structure. Figure 1 shows the magnitude and frequency spectrum of the external axial magnetic field B_e, measured by a magnetic loop surrounding the quartz vessel wall at the midplane. Also shown in the figure is the amplitude of the applied RMF vacuum field B_ω, which decays by about a

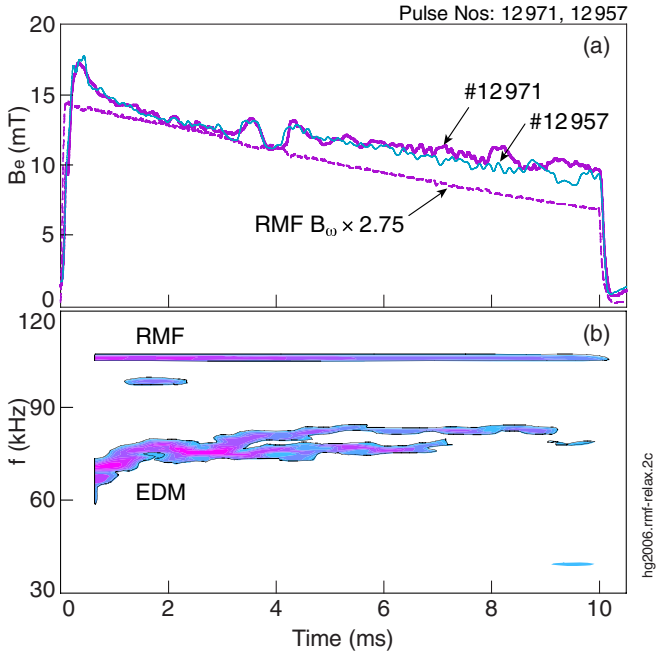

FIG. 1 (color online). (a) Evolution of external axial magnetic field B_e and applied RMF vacuum field B_ω for a typical long pulse FRC sustained by RMF, #12 971. Time trace of B_e for #12 957 is also shown to illustrate the reproducibility. (b) Spectrogram of B_e for #12 971, showing a clear change in mode structure upon transition to a high-confinement state, as signified by the sudden rise in B_e.

factor of 2 during the pulse mainly due to losses in the RMF pulser tubes. Nevertheless, the full FRC is maintained for the entire RMF duration, over 100 overall resistive decay times.

As can be seen, the initial transition to the high-confinement state occurs at ~3.5 ms, with plasma settled down after a brief transitory period. The B_e spectrogram shows two dominant oscillations: one at the applied RMF frequency $f_\omega \sim 105$ kHz, and another at a downshifted frequency $f_d \sim 75$ kHz, caused by what has been termed an "edge driven mode" (EDM) [13]. The EDM is produced by the tearing and reconnection between the external applied RMF and the inner RMF ($r < R =$ radius of magnetic axis), which is frozen into the electron fluid, at frequency $f_d = f_\omega - f_e$, with f_e being the electron rotation frequency. The continuous tearing and reconnection between the outer and inner RMF modulates the applied RMF torque, thus resulting in a perturbation in FRC flux and magnetic field at frequency f_d. Upon transition to the high-confinement state, the EDM splits into two separate modes; this represents a bifurcation in electron rotation.

Figure 2 shows the detailed frequency spectrum of the axial magnetic fields B_z, measured by a multichannel internal magnetic probe oriented to pick up only the axial magnetic field, for the time periods (over 1 ms) before and after the transition to the high-confinement state. The probe contains 31 magnetic pick-up loops with the first 11 loops (2-cm apart) covering $r = 0$ to $r = 20$ cm and the remaining 20 loops (1-cm apart) covering $r = 21$ to $r = 40$ cm. Before the transition, the EDM is the dominant mode in the discharge, producing strong magnetic perturbations close to the geometric axis ($r = 0$). Some $n = 2$ oscillations appear outside the field null, but with much smaller amplitude. After the transition, the $n = 2$ mode disappears, and the oscillations at the original EDM frequency fall dramatically. It is interesting to note that significant oscillations appear at frequencies near the electron drift frequencies $f_{e1} \sim 23$ kHz and $f_{e2} \sim 30$ kHz. The lower-frequency (f_{e1}) oscillations spread over a broad region with maximum amplitude well inside the field null ($R \sim 0.25$ m), while the higher-frequency (f_{e2}) oscillations are more concentrated in the outer region. The EDM only accounts for the $\tilde{B}_z$ oscillations at $f_d = f_\omega - f_e$, i.e., around 80 kHz, but *not* those at low frequencies.

Since the FRC is a diamagnetic entity with the current perpendicular to the magnetic field throughout the plasma, drift waves are a basic feature of such a configuration. Krall has postulated that in elongated FRCs, high-β, low-frequency electromagnetic drift waves exist, with frequency $\omega_{\mathrm{LFD}} \sim k_\theta V_d$, where k_θ is the azimuthal wave number, $V_d = T_i/(eB\lambda_n)$, and λ_n is the density gradient scale length inside the separatrix [7]. In contrast to low-β, electrostatic drift waves (universal instabilities), this class of modes is predominantly *electromagnetic*, thus producing magnetic field compression. We surmise that the observed low-frequency oscillations are indicative of the presence of these LFD instabilities. Assuming a usual rigid-rotor (RR) profile for a FRC, for $n = 1$ and $k_\theta =$

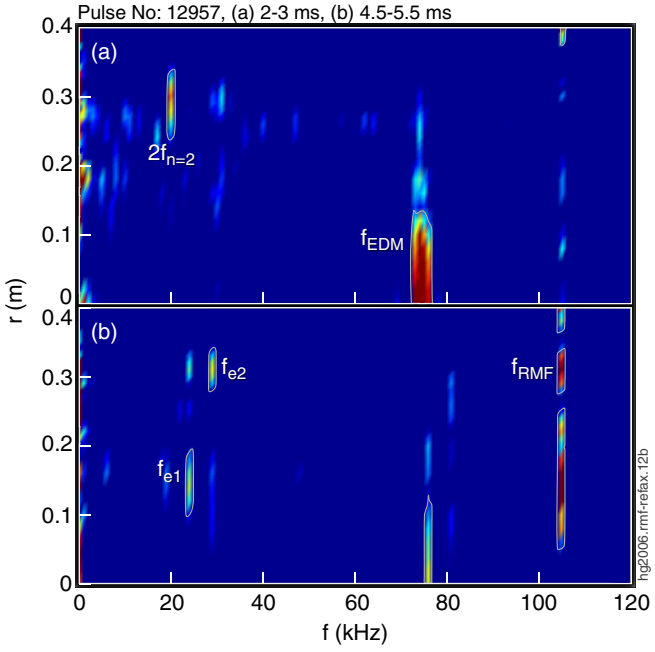

FIG. 2 (color online). Radial contours of the frequency spectrum of B_z for the time periods: (a) before the transition (2–3 ms), and (b) after the transition (4.5–5.5 ms). Some significant modes are highlighted.

$1/r$, $f_{\mathrm{LFD}} = \omega_{\mathrm{LFD}}/2\pi = \frac{4K_{\mathrm{RR}}}{\pi r_s^2} \cdot \frac{T_i}{eB_e}$, where K_{RR} is the RR parameter, and r_s is the separatrix radius. The RMF-sustained FRCs in TCS exhibit a "double-RR" profile with $K_{\mathrm{RR}} \sim 1.5$ for $r > R$ and $K_{\mathrm{RR}} \sim 1.0$ inside [14]. This type of behavior might be expected during RMF drive since unsustained FRCs tend to have uniform f_e, but the RMF drive produces higher values of f_e near the separatrix. Using $r_s \sim 0.35$ m, $T_i \sim T_e \sim 20$ eV, and $B_e \sim 10$ mT, then $f_{\mathrm{LFD}} \sim 31$ kHz for $r > R$, and ~21 kHz for $r < R$ in the inner region, consistent with the experimental observations.

A truly remarkable feature is that the transition to the high-confinement state dramatically alters the structure of the applied RMF. A new RMF $\tilde{b}_z$ appears, as evidenced by the strong oscillations at $f_\omega \sim 105$ kHz both inside and outside $r = R$. The $\tilde{b}_z$ oscillations are by far the strongest oscillations in the axial magnetic field. This does not suggest an internal tilt mode, since the applied RMF ($\tilde{b}_\theta$ and $\tilde{b}_r$) appears predominantly for $r > R$, while strong $\tilde{b}_z$ oscillations also appear over a broad region for $r < R$. This self-developed $\tilde{b}_z$ field, in all probability, arises from a change in the global magnetic topology. Magnetic topology changes are a marker of the relaxation process. The resulting screen current $\tilde{j}_\theta$, coupled with radial RMF $\tilde{b}_r$, would, in turn, drive a steady poloidal current by the $\langle \tilde{j}_\theta \tilde{b}_r \rangle$ force, in addition to the normally driven toroidal current, thus sustaining the magnetic helicity.

Further evidence of relaxation is manifested by the spontaneous development of a *steady* toroidal field B_θ near the magnetic axis during the transition. The transition to the high-confinement state is always accompanied by a jump in a steady toroidal field, with a peak magnitude up to 1/4 the poloidal field at the separatrix. The toroidal field is usually maintained for up to 150 axial Alfvén times, i.e., ~2 ms, after the plasma settles into the high-confinement state, then slowly reverses its direction. Self-generated toroidal fields have usually been observed in RMF-driven FRCs in rotamak experiments, however with opposite signs of the fields in the two hemispheres [15,16]. This could be related to the specific rotamak topology where the applied RMF provides naturally a rotating field $\tilde{b}_\phi$ along the spherically shaped plasma boundary, with reversed field direction in each hemisphere, in addition to $\tilde{b}_r$ and $\tilde{b}_\theta$ (in spherical coordinates) [15], or generated by poloidal swirling electron flows around the FRC ends [16]. Having only internal field measurements at the midplane of TCS, the question is—does the observed toroidal field merely reflect an axial shift of the FRC so that the probes pick up the toroidal fields at one half of the FRC? However, inspection of the axial structure of the diamagnetism vs time shows that the FRC *does not* shift axially during the transition. Furthermore, the improvement in performance occurs over the entire FRC column.

Figure 3(a) shows the detailed $B_z(r)$ and $B_\theta(r)$ profiles obtained from the internal probe right after the transition, along with predictions from various models to be discussed later. A notable feature is that the toroidal field is localized near the field null in the region where the poloidal confinement field is small. The B_θ structure near $r = R$ resembles that anticipated in a force-free ($\boldsymbol{J} \parallel \boldsymbol{B}$) relaxed state, as in spheromaks and reversed field pinches. To examine such an intriguing possibility, Fig. 3(a) also shows the field profiles for a force-free state [1], as represented by the Bessel function model: $B_z/B_{z0} = \alpha J_0(r/r_s)$ and $B_\theta/B_{z0} = -\alpha J_1(r/r_s)$, where α is a constant. These profiles, with $\alpha = 0.7$ chosen, indeed, provide a reasonable fit to the experimental measurements in the core region. Figure 3(b) shows the corresponding pressure profile deduced from the measured internal field profiles and radial force balance, taking into account the radial force $\langle \tilde{j}_z \tilde{b}_\theta \rangle$ from the RMF, $\frac{dp}{dr} = -\frac{B_\theta}{\mu_0 r}\frac{d(rB_\theta)}{dr} - \frac{B_z}{\mu_0}\frac{dB_z}{dr} - \langle \tilde{j}_z \tilde{b}_\theta \rangle + n_i m_i \frac{u_\theta^2}{r}$, where $p = p_i + p_e$ is the total pressure, and u_θ is the ion toroidal rotation speed, as obtained from multichannel ion Doppler spectroscopy. For comparison, the figure also shows a pressure profile before the transition (at 2.5 ms). As can be seen, after the transition, the pressure is nearly constant in the region near the magnetic axis, further indicating a near-force-free state in the core of the FRC.

The possible significance of the self-generated toroidal field in the RMF-sustained FRCs is illustrated by its connection with the safety factor, which is a common index of

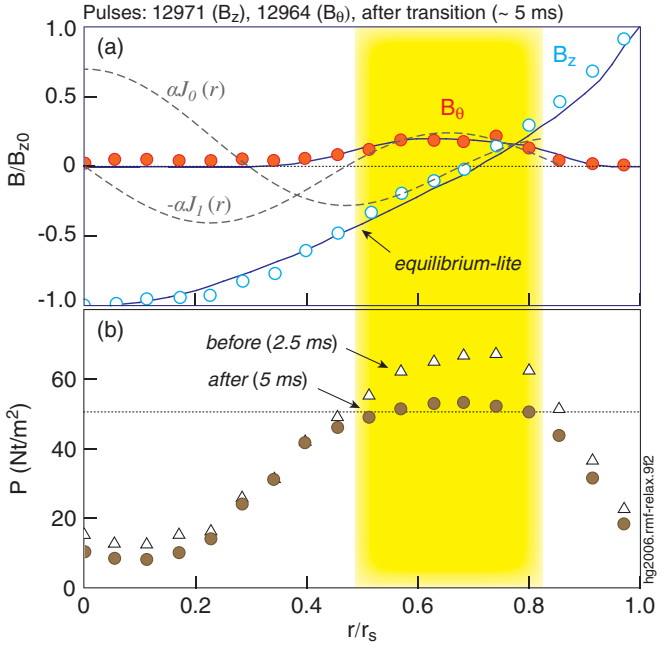

FIG. 3 (color online). (a) Radial profiles of axial (poloidal) and toroidal fields, $B_z(r)$ and $B_\theta(r)$, right after the transition to the high-confinement state. Data points are obtained from internal probe measurements. Dashed lines indicate Bessel solutions of a force-free ($\boldsymbol{J} \parallel \boldsymbol{B}$) plasma state, providing a reasonable fit to the data in the core region. Solid lines represent the equilibrium-lite model. (b) Pressure profiles before and after the transition.

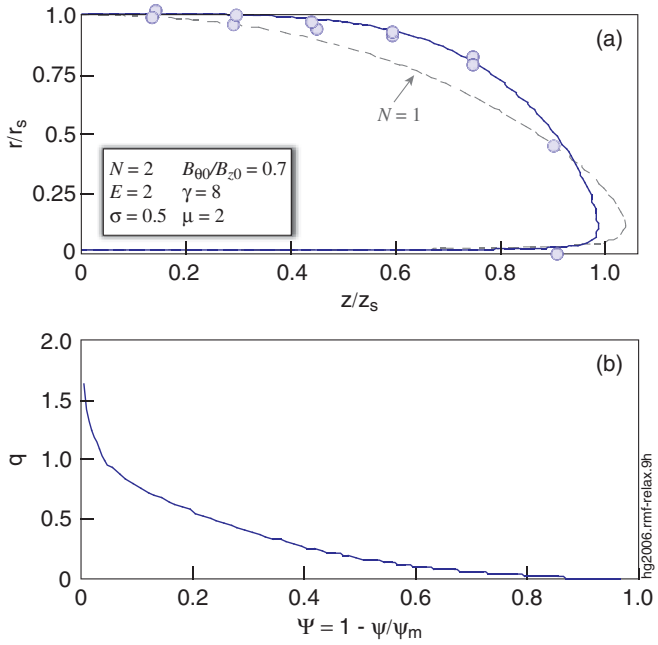

FIG. 4 (color online). (a) Axial structure of the FRC calculated by the equilibrium-lite model (solid line), with the model input parameters also indicated in the figure, and the shape of the separatrix inferred from the excluded flux radius measurements (symbols). For comparison, the separatrix shape predicted by the model with $N = 1$ is also shown. (b) q profile derived from the measured internal fields plotted against the normalized flux $\Psi = 1 - \psi/\psi_m$, $\Psi = 0$ at the magnetic axis, and $\Psi = 1$ at the edge.

stability in magnetic fusion plasmas. For determining the q profile, we have developed a 2D equilibrium-lite model. This model employs a multiparameter analytic structure for the magnetic fields, extrapolating from the Hill's vortex equilibrium [4,17]. For poloidal field structure, we consider a quasiequilibrium with

$$\psi = (1/2)B_{z0}r^2 f, \tag{1}$$

where $f \equiv (1-\rho)[1-2(1-\sigma)\rho(1-\rho)] - (z/z_s)^{2N}$, and $\rho \equiv (r/r_s)^2$. Here z_s is the separatrix half-length, so that the separatrix elongation is $E = z_s/r_s$. Note that the Hill's vortex is recovered if the profile parameters $N = 1$, $\sigma = 1$. Here N serves as a "racetrack" parameter. For $N = 1$ and $\sigma = 1$ the separatrix ($\psi = 0$ surface) is elliptical. If $N > 1$ the separatrix is racetracklike, although the degree of racetrackness is also influenced by σ. The parameter σ measures the current density at the field null relative to that in the Hill's vortex. In particular, for $\sigma < 1$, the current density profile is *hollow*, i.e., j_θ is depressed, and the magnetic field gradient is flattened in the neighborhood of the field null, which is a unique feature of the RMF-sustained FRCs in TCS. In addition, a particular toroidal field structure is adopted to represent that observed in the TCS-RMF experiments, i.e., rather localized in the neighborhood of the field null, with

$$B_\theta = B_{\theta 0} r f \exp\{-\gamma[2(r/r_s)^2 - 1]^{2\mu}\}. \tag{2}$$

The B_z and B_θ profiles obtained from the model are shown in Fig. 3(a) as solid lines. The axial structure of the FRC is shown in Fig. 4(a), together with the excluded flux radius measurements. A reasonable fit is obtained with $N = 2$ (solid line), in contrast to an elliptical ($N = 1$) separatrix shape (dashed line). The corresponding q profile is shown in Fig. 4(b). Notably, a significant $q \sim 1$ appears near the magnetic axis along with significant magnetic shear. These features should improve stability and confinement in the core.

In summary, spontaneous transition to a high-confinement state appears in RMF-sustained high-β FRCs, accompanied by the development of a small toroidal field. This self-organized compact toroid exhibits a near-force-free state in the neighborhood of the magnetic axis, providing the first evidence for relaxation in steady-state high-β plasmas. Low-frequency drift modes are identified as the dominant instabilities during the transition, and may be associated with the relaxation process. Although the self-generated toroidal field is small, it leads to $q \sim 1$ and significant magnetic shear in the core of the FRC, as a result of the high elongation and small aspect ratio. This may promote good stability and confinement, as observed in TCS.

Thanks are given to the rest of the RPPL staff. Helpful discussions with T. R. Jarboe are also acknowledged. This work was funded by the U. S. Department of Energy.

[1] J. B. Taylor, Phys. Rev. Lett. **33**, 1139 (1974).
[2] L. C. Steinhauer and A. Ishida, Phys. Rev. Lett. **79**, 3423 (1997).
[3] Z. Yoshida and S. M. Mahajan, Phys. Rev. Lett. **88**, 095001 (2002).
[4] H. Y. Guo *et al.*, Phys. Rev. Lett. **92**, 245001 (2004).
[5] H. Y. Guo *et al.*, Phys. Rev. Lett. **95**, 175001 (2005).
[6] A. L. Hoffman *et al.*, Nucl. Fusion **45**, 176 (2005).
[7] N. A. Krall, Phys. Fluids **30**, 878 (1987).
[8] H. A. Blevin and P. C. Thonemann, Nucl. Fusion Suppl. Part I, 55 (1962).
[9] W. N. Hugrass *et al.*, Phys. Rev. Lett. **44**, 1676 (1980).
[10] I. R. Jones, Phys. Plasmas **6**, 1950 (1999).
[11] A. L. Hoffman *et al.*, Fusion Sci. Technol. **41**, 92 (2002).
[12] H. Y. Guo *et al.*, Phys. Rev. Lett. **94**, 185001 (2005).
[13] R. D. Milroy and K. E. Miller, Phys. Plasmas **11**, 633 (2004).
[14] A. L. Hoffman *et al.*, Phys. Plasmas **13**, 012507 (2006).
[15] S. Xu and I. R. Jones, Plasma Phys. Controlled Fusion **35**, 531 (1993).
[16] Y. Petrov *et al.*, Phys. Plasmas **12**, 082514 (2005).
[17] L. C. Steinhauer *et al.*, Phys. Plasmas **13**, 056119 (2006).